Digest Journal of Nanomaterials and Biostructures Vol. 14, No. 3, July - September 2019, p. 593 - 599

SONOCHEMICAL SYNTHESIS AND CHARACTERIZATION OF BiOCl NANOPLATES AND THEIR PHOTODEGRADATION OF RHODAMINE B

P. INTAPHONG[a], A. PHURUANGRAT[a,*], K. KARTHIK[b], T. THONGTEM[c,d]
S. THONGTEM[c,e]
[a]*Department of Materials Science and Technology, Faculty of Science, Prince of Songkla University, Hat Yai, Songkhla 90112, Thailand*
[b]*School of Physics, Bharathidasan University, Tiruchirappalli 620 024, India*
[c]*Materials Science Research Center, Faculty of Science, Chiang Mai University, Chiang Mai 50200, Thailand*
[d]*Department of Chemistry, Faculty of Science, Chiang Mai University, Chiang Mai 50200, Thailand*
[e]*Department of Physics and Materials Science, Faculty of Science, Chiang Mai University, Chiang Mai 50200, Thailand*

BiOCl nanoplates were successfully synthesized by a simple sonochemical method at the pH of 2–12. The effect of pH of precursor on phase, morphologies and photocatalytic reaction of BiOCl was investigated in this research. X-ray diffraction (XRD), scanning electron microscopy (SEM) and transmission electron microscopy (TEM) revealed the presence of pure tetragonal BiOCl phase with different morphologies (nanoplates, mesoporous hierarchical flowers of nanoplate petals and flowers-nanoplates mixture). The photocatalytic activities of the BiOCl nanoplates were evaluated through the degradation of rhodamine B (RhB) under visible-light irradiation. They were found that mesoporous hierarchical BiOCl flowers synthesized at the pH of 6 showed the highest photodegradation efficiency of 96.24 % within 20 min.

(Received April 21, 2019; Accepted July 20, 2019)

Keywords: BiOCl, Rhodamine B, Photocatalysis

1. Introduction

Contamination in industrial has become a major environmental concern. Organic dyes are significant parts of industrial byproducts. These dyes have been found to have great hazardous effects not only on human's health but also adversely affect aquatic lives and the environmental surrounding. The dangerous effects of these organic pollutants become apparent when they contain in natural water. Therefore, the best way or technique that can effectively degrade these pollutants is developed before they are released into the environment [1–3]. Consequently, a number of conventional techniques such as biodegradation, adsorption and advanced oxidation processes have been developed to manage the problem of industrial waste. Nevertheless, these methods are not able to completely degrade pollutants [3–5].

The photocatalytic degradation of organic pollutants is expected as an important method used to solve environmental problems. According to the previous reports, the performance of these photocatalytic materials is closely related to their microstructure, composition, particle size, morphology, etc. Conventional photocatalysts with wide band gaps such as TiO_2 and ZnO have limited performance to degrade organic pollutants due to their wide band gaps that confine their operational range to the ultraviolet region which accounts for 5 % of the solar radiation [6–8]. Moreover, they have rapid recombination of photo-induced electron-hole pairs that leads to low photodegradation efficiency and no absorption of visible light irradiation. Thus the main purpose is to focus on the development of photocatalyst with highly efficient activity.

* Corresponding author: phuruangrat@gmail.com

Recently, bismuth oxyhalides (BiOX, X=Cl, Br, I) are candidates for photodegradation of organic pollutants because of their catalytic properties. All the BiOX compounds have unique layered structure, composed of $[Bi_2O_2]$ slabs interleaved by double slabs of X atoms.This layered structure can effectively induce the separation of photo-induced electron–hole pairs [9–11]. BiOX shows excellent photocatalytic properties in eliminating of organic pollutants under visible light irradiation. Among the BiOX compounds, BiOCl with its band gap energy of 2.3 eV can respond to visible light irradiation (48 % of solar radiation) and shows excellent photocatalytic properties. Lately, ultrasonic irradiation has achieved much attention because it can cause physical and chemical changes through ultrasonic cavitation such as growth rate, rapid formation and collapse of unstable bubbles in liquid. This method produced nanoparticles and required short time period [12].

In this work, BiOCl photocatalyst was synthesized by sonochemical method in solutions with different pH values. The structure, morphology and photocatalytic properties of as-synthesized BiOCl were investigated by different characterization techniques. Photocatalytic activities of as-synthesized BiOCl samples were evaluated by photodegradation of rhodamine B (RhB) under visible light irradiation.

2. Experimental procedure

To form a set of solutions, each 0.01 mole of $Bi(NO_3)_3$ and NaCl was dissolved in 100 ml RO water under vigorous stirring until complete dissolution. Then, 3 M NaOH solution was slowly dropped to these solutions to adjust the pH of 2–12. The solutions were processed in ultrasonic bath at 80 ^oC for 5 h. The precipitates were collected and dried at 100 ^oC for 24 h for further characterization.

Crystalline phase of the as-synthesized samples was characterized by an X-ray diffractometer (XRD, Philips X'Pert MPD) with Cu K_α radiation in the 2θ range of 10–60°. The morphologies and microstructures were characterized by a scanning electron microscope (SEM, JEOL JSM 6335 F) operating at 20 kV and a transmission electron microscope (TEM, JEOL JEM-2010) operating at 200 kV.

The photocatalytic activities of the as-synthesized products were evaluated by measuring the degradation of rhodamine B (RhB) in an aqueous solution under visible light radiation of Xe light source. The 200 mg photocatalyst was suspended in a 200 ml of $1x10^{-5}$ M RhB aqueous solution. Subsequently, the solution was magnetically stirred for 30 min in the dark to establish an adsorption/desorption equilibrium of RhB on the photocatalytic surface. Then, the visible light was turned on to initiate the photocatalysis. The solution was analyzed by a Perkin Elmer Lambda 25 spectrometer using a 450 W Xe lamp with 554 nm wavelength. The decolorization efficiency was calculated using the equation

$$\text{Decolorization efficiency (\%)} = \frac{C_o - C_t}{C_o} \text{ x } 100 \quad (1)$$

, where C_o is the initial concentration of RhB and C_t is the concentration of RhB after visible light irradiation within a period of time t.

3. Results and discussion

XRD patterns in $2\theta = 10^o–60^o$ of as-synthesized BiOCl samples as visible-driven photocatalyst synthesized in solutions with different pH by sonochemical method are shown Fig. 1. XRD patterns of all as-synthesized BiOCl samples can be indexed to the tetragonal phase of BiOCl (JCPDS No. 06-0249) belonging to the (001), (002), (101), (110), (102), (111), (003), (112), (200), (113), (211), (104) and (212) planes [13]. They can be seen that the intensity and sharpness of diffraction peaks of BiOCl samples were decreased with increasing in the pH of the

solution precursors from pH 2 to pH 12, indicating that the degree of crystallinity of the products was decreased for the formation of BiOCl at high pH. Furthermore, the diffraction peaks of the as-synthesized BiOCl at low pH possess intense and narrow diffraction peaks, suggesting the products are good crystal [14]. No other impurities were detected, indicating that BiOCl products have high purity and are single phase. Furthermore, the relative intensities of all (001) facets in XRD patterns of products are higher than the intensity of the (001) facet of JCPDS No. 06-0249 as standard, indicating the growth of BiOCl samples is in highly exposed (001) facet [15]. It is well known that highly exposed (001) face in BiOX (X = Br, Cl, I) favors the separation of photo-induced charge carriers which enhance the photocatalytic reaction of BiOX under visible light irradiation [15]. Therefore, the XRD analysis confirms that pure phase and high crystalline as-synthesized BiOCl samples as visible-light-driven photocatalyst have been successfully synthesized by a novel facile sonochemical method in the solutions with the pH of 2–12.

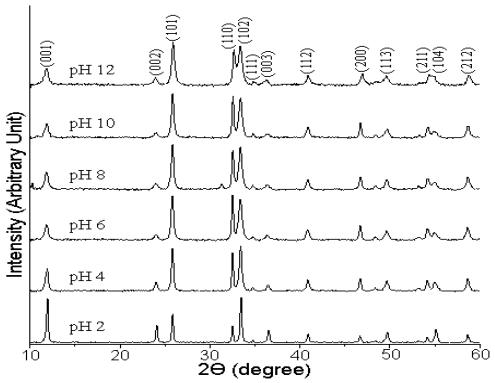

Fig. 1 XRD patterns of BiOCl photocatalysts synthesized in the solutions with the pH of 2, 4, 6, 8, 10 and 12 by sonochemical method.

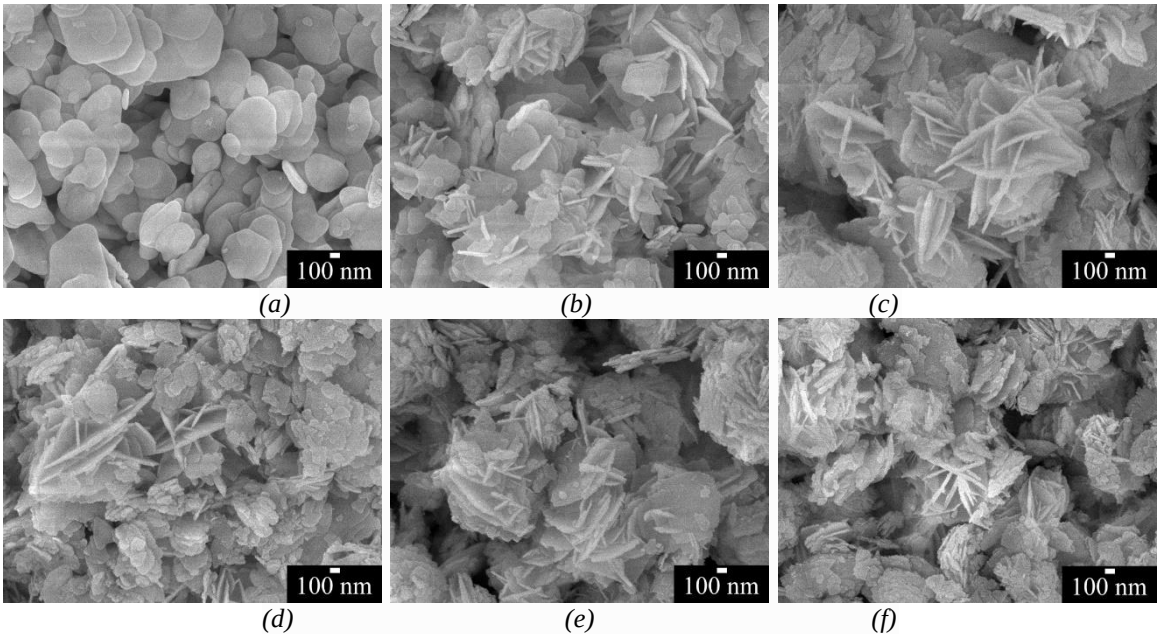

Fig. 2 SEM images of BiOCl synthesized in the solutions with different pH of (a) 2, (b) 4, (c) 6, (d) 8, (e) 10 and (f) 12 by sonochemical method.

Morphologies of as-prepared BiOCl samples with different pH were investigated by SEM as the results shown in Fig. 2. SEM images of all BiOCl samples show different size and thinness of nanoplates with average size of 400–550 nm. At pH 2, BiOCl sample shows an individual

nanoplate with 100–300 nm diameter and 50–60 nm thick. Formation of agglomerate nanoplate colonies was detected at the pH 4. Upon increasing the pH to 6, the BiOCl nanoplates were assembled to mesoporous hierarchical BiOCl flowers with nanoplates as petals. The nanopetals are ~10 nm thick and ~200 nm in plane size. Each mesoporous hierarchical BiOCl flower was built from connecting nanoplates around the same center. Yang et al. reported that Bi_2WO_6 hierarchical microspheres showed faster and higher efficiency for photodegradation of rhodamine B (RhB) under visible light irradiation [16]. Enhanced photocatalytic activity of Bi_2WO_6 hierarchical microspheres is due to the larger specific surface area that provides more surface active sites and enhances charge carrier diffusion. In the basic solutions (pH=8–12), some of petals of mesoporous hierarchical BiOCl flowers were loosen and transformed into clusters of BiOCl nanoplates. This observation reveals that pH of precursor is the key parameter in synthesizing of BiOCl with controlled morphologies by sonochemical method at room temperature, as visible-light-driven photocatalyst with enhanced photocatalytic activity for degradation of RhB under visible light irradiation [17–19].

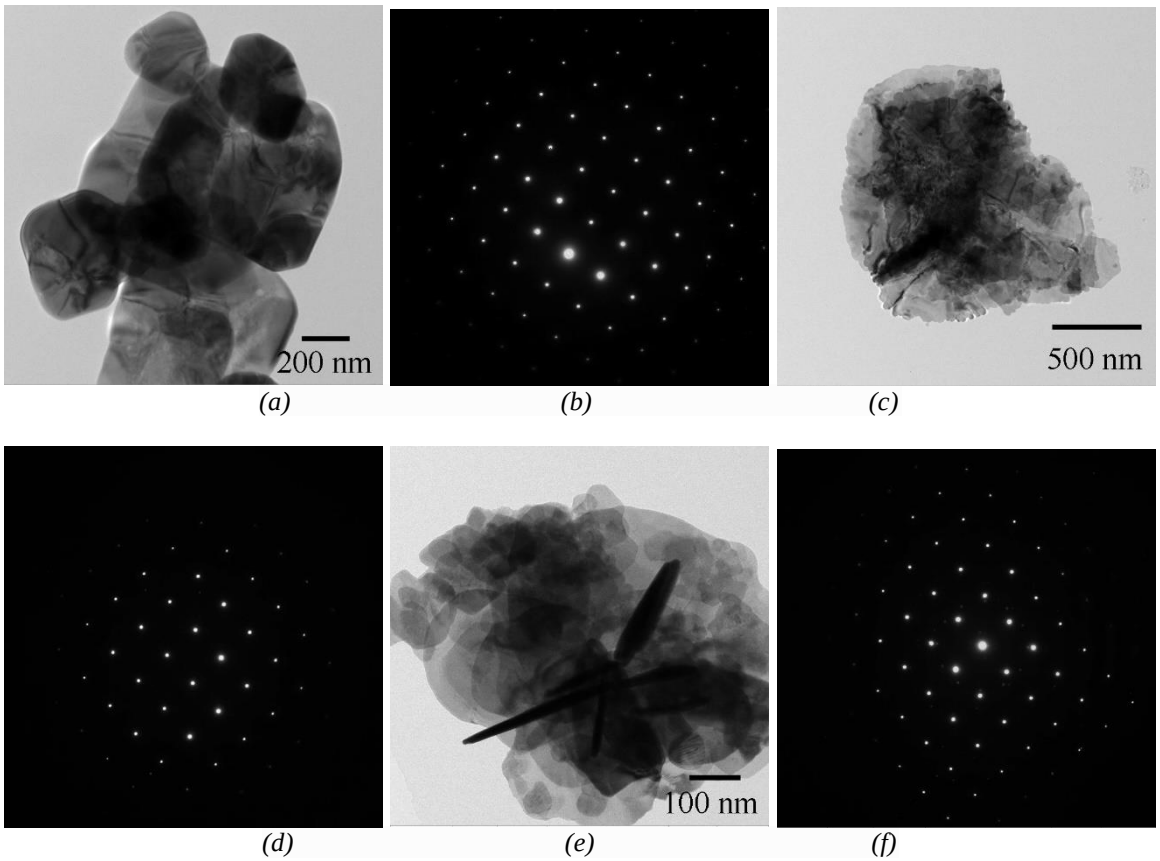

Fig. 3 TEM images and SAED patterns of as-synthesized BiOCl products as visible-light-driven photocatalyst by sonochemical method using different pH of (a and b) 2, (c and d) 6 and (e and f) 10.

Morphologies and phase of as-prepared BiOCl samples at pH 2, 6 and 10 were investigated by TEM and SAED as the results shown in Fig. 3. TEM image revealed that as-prepared BiOCl sample at the pH 2 is composed of nanoplates with the diameter of 200–600 nm, in good accordance with the above SEM observation. The surface of BiOCl nanoplates is smooth. SAED pattern of a single prepared BiOCl nanoplate appears as white spot electron diffraction pattern, certifying that the product is single crystal. It can be indexed to the (100), (110) and (010) planes for tetragonal BiOCl phase with zone axis of [001]. By increasing the pH of precursor solution to 6, TEM image of product shows gradually assembled nanoplates of mesoporous

hierarchical BiOCl flowers. The size and thickness of the nanoplate petals were simultaneously reduced comparing to the BiOCl nanoplates at the pH 2. The SAED pattern of a single nanoplate of mesoporous hierarchical BiOCl flowers presented only the single crystalline tetragonal BiOCl phase. The pure BiOCl sample at the pH 10 presented mixed morphologies of mesoporous hierarchical BiOCl flowers with the diameter of 400–600 nm as the majority and clusters of BiOCl nanoplates with the diameter of 100–200 nm as the minority. The thinness of nanoplates of hierarchical BiOCl flowers at the pH 6 and 10 is less than that of the BiOCl nanoplates at the pH 2. Thus they can absorb more visible light irradiation and have higher photocatalytic efficiency. The SAED patterns of BiOCl at the pH 6 and 10 presented spots of electron diffraction which certified that the products are single crystalline BiOCl phase. The angles labeled in the SAED patterns are 45^{o} and 90^{o}, in agreement with the theoretical value of the angle between the (110) and (200) planes and (110) and (1-10) planes with [001] zone axis of tetragonal BiOCl phase.

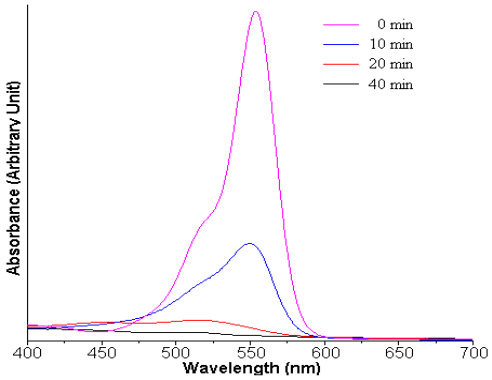

Fig. 4 Temporal evolution of visible light irradiation for absorbance of RhB solution over BiOCl as photocatalyst synthesized in the solution with the pH of 6.

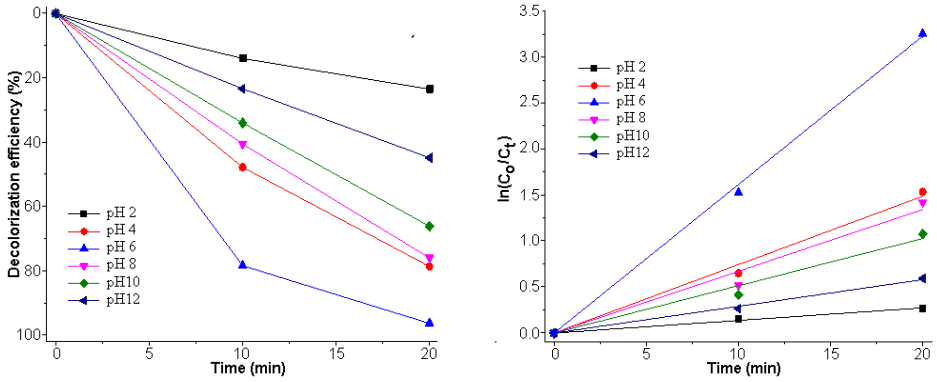

(a) *(b)*

Fig. 5(a) Photocatalytic degradation and (b) the plots of $ln(C_o/C_t)$ for different lengths of time by BiOCl synthesized at the pH of 2, 4, 6, 8, 10 and 12.

Photocatalytic activities of the as-synthesized BiOCl samples were investigated by photodegradation of RhB as model dye solution under visible light irradiation. Fig. 4 shows the absorption spectral change accompanying the photodegradation of RhB solution by the as-synthesized BiOCl at the pH of 6 under visible light irradiation. The RhB solution showed a maximum absorption (λ_{max}) at 554 nm wavelength, which rapidly decreased with the temporal evolution of light irradiation. The absorbance was completely stationary within 40 min and the color of solution gradually transformed from pink into paler color and finally into colorless and transparent solution, suggesting that RhB molecules were completely decomposed. At the conclusion of 40 min irradiation, λ_{max} of RhB was blue-shift to 498 nm caused by N-deethylation

of RhB during reaction [18, 19]. The resultants of N-deethylation of RhB contain N,N,N′-triethyl rhodamine (539 nm), N,N′-diethyl rhodamine (522 nm), N-ethyl rhodamine (510 nm) and rhodamine (498 nm) [22].

Fig. 5a shows the photocatalytic activities of different visible-light-driven BiOCl photocatalysts in degradation of RhB under visible light irradiation ($\lambda > 420$ nm) within 20 min. The photocatalytic activity of BiOCl synthesized at the pH 6 shows the highest photocatalytic performance of almost 96.24 % under visible light within 20 min. According to the experimental results, photocatalytic activity of BiOCl is controlled by the morphology of product. The higher photocatalytic activity of hierarchical BiOCl flowers with nanoplate petals is due to their larger specific surface area that provides more surface active sites and enhances charge carrier diffusion [16]. The kinetics of RhB degradation by the visible-light-driven BiOCl photocatalysts under visible light irradiation ($\lambda > 420$ nm) within 20 min were studied using pseudo-first-order model in term of the Langmuir–Hinshelwood model as follows.

$$\ln(C_0/C_t) = kt \quad (2)$$

, where k is the apparent rate constant, C_o and C_t are the concentrations of dye in solutions at irradiation time of 0 and t, respectively [16, 23, 24]. Fig. 5b shows the plotting graphs of $\ln(C_o/C_t)$ versus irradiation time of RhB photodegradation by BiOCl photocatalyst synthesized in the solutions with different pH. The linearity observed in the kinetic plots expressed as $\ln(C_o/C_t)$ versus irradiation time, which certifies that the degradation reaction follows the first-order kinetics model. The apparent rate constant can be determined from the slope of the linear plot. Through this model, the calculate reaction rate constants of BiOCl are 0.0133, 0.0769, 0.1639, 0.0710, 0.0539 and 0.0297 min^{-1} for as-synthesized BiOCl samples at the pH 2, 4, 6, 8, 10 and 12, respectively. In this research, BiOCl synthesized at the pH of 6 exhibited the highest apparent rate constant. Clearly, BiOCl at the pH 6 shows the highest photocatalytic rate for degradation of RhB dye solution stimulated by visible radiation [23, 24].

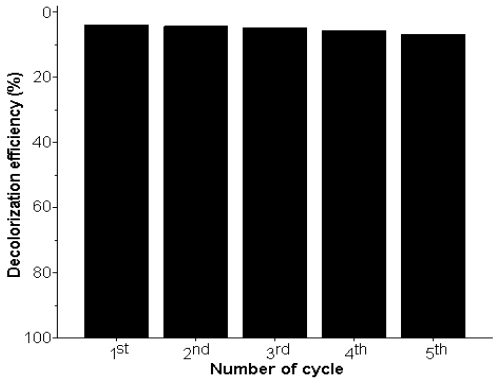

Fig. 6 Photocatalytic degradation of RhB for five re-cycles of the re-used BiOCl synthesized at the pH 6.

In order to determine the recyclability of the reused BiOCl synthesized at the pH 6, photocatalysis was carried out under same condition. At the end of each photocatalytic cycle, BiOCl at the pH 6 as photocatalyst was centrifuged, washed with distilled water and ethanol, and dried at 100 °C for 24 h. The photocatalytic activity of the as-prepared BiOCl at the pH 6 still maintain high performance for photocatalytic reaction even at the end of the 5^{th} cycle as the results shown in Fig. 6. The recycled test indicated that BiOCl at the pH 6 has high photostability during photocatalytic test. The photodegradation efficiency of BiOCl at the end of the fifth cycle is 93.42 % which is slightly decreased as compared to that of the first cycle due to the residual RhB adsorbed on the surface of the catalyst. Therefore, BiOCl synthesized at the pH 6 is an effective and stable photocatalyst for degradation of dye in wastewater under visible light irradiation.

4. Conclusions

BiOCl photocatalysts were successfully synthesized by sonochemical method. The pure tetragonal BiOCl phase was obtained in the solutions with the pH 2–12. The as-synthesized mesoporous hierarchical BiOCl flowers at the pH of 6 showed the highest photodegradation efficiency of 96.24 % within 20 min because their larger specific surface area provides more surface active sites and enhances charge carrier diffusion.

Acknowledgement

We are extremely grateful to the Prince of Songkla University, Hat Yai, Songkhla 90112, Thailand for providing financial support through the contact no. SCI620121S.

References

[1] G. Li, F Qin, R. Wang, S. Xiao, H. Sun, R. Chen, J. Colloid. Interf. Sci. **409**, 43 (2013).
[2] H. Li, J. Liu, T. Hu, N. Du, S. Song, W. Hou, Mater. Res. Bull. **77**, 171 (2016).
[3] A. M. Alansi a, M. Al-Qunaibit, I. O. Alade, T. F. Qahtan, T. A. Saleh, J. Mol. Liq. **253**, 297 (2018).
[4] K. Natarajan, H. C. Bajaj, R.J. Tayade, J. Ind. Eng. Chem. **34**, 146 (2016).
[5] M. Jabli, N. Tka, K. Ramzi, T.A. Saleh, J. Mol. Liq. **249**, 1138 (2018).
[6] M. He, W. Li, J. Xia, L. Xu, J. Di, H. Xu, S. Yin, H. Li, M. Li, Appl. Surf. Sci. **331**, 170 (2015).
[7] H. Li, Q. Jia, Y. Cui, S. Fan, Mater. Lett. **107**, 262 (2013).
[8] D. Wu, S. Yue, W. Wang, T. An, G. Li, H. Yip, H. Zhao, P. Wong, Appl. Cata. B **192**, 35 (2016).
[9] Z. Liu, B. Wu, Mater. Sci. Semicond. Process. **31**, 68 (2015).
[10] X. Qin, H. Cheng, W Wang, B. Huang, X. Zhang, Y. Dai, Mater. Lett. **100**, 285 (2013).
[11] J. Li, S. Sun, C. Qian, L. He, K. K. Chen, T. Zhang, Z. Chen, M. Ye, Chem. Eng. J. **297**, 139 (2016).
[12] C. Yang, F. Li, T. Li, W. Cao, J. Mol. Catal. A **418–419**, 132 (2016).
[13] Powder Diffract. File, JCPDS-ICDD, 12 Campus Bld., Newtown Square, PA 19073-3273, U.S.A. (2001).
[14] J. Song, Q. Fan, W. Zhu, R. Wang, Z. Dong, Mater. Lett. **165**, 14 (2016).
[15] H. Li, Z. Yang, J. Zhang, Y. Huang, H. Ji, Y. Tong, Appl. Surf. Sci. **423**, 1188 (2017).
[16] A. M. Yang, Y. Han, S. S. Li, H. W. Xing, Y. H. Pan, W. X. Liu, J. Alloy. Compds. **695**, 915 (2017).
[17] J. Zhang, J. Wu, P. Lu, Q. Liu, T. Huang, H. Tian, R. Zhou, J. Ren, B. Yuan, X. Sun, W. Zhang, Mater. Lett. **186**, 353 (2017).
[18] L. Ye, Y. Su, X. Jin, H. Xie, F. Cao, Z. Guo, Appl. Surf. Sci. **311**, 858 (2014).
[19] F. Dong, Y. Sun, M. Fu, Z. Wu, S.C. Lee, J. Hazard. Mater. **219-220**, 26 (2012).
[20] Y. Li, Y. Tian, R. Zhang, L. Ma, C. Zhou, X. Tian, Inorg. Chim. Acta. **439**, 123 (2016).
[21] J. Xia, J. Zhang, S. Yin, H. Li, H. Xu, L. Xu, Q. Zhang, J. Phys. Chem. Solids **74**, 298 (2013).
[22] X. Hao, J. Zhao, Y. Zhao, D. Ma, Y. Lu, J. Guo, Q. Zeng, Chem. Eng. J. **229**, 134 (2013).
[23] L. Song, Y. Pang, Y. Zheng, C. Chen, L. Ge, J. Alloy. Compd. **710**, 375 (2017).
[24] Y. Cai, D. Li, J. Sun, M. Chen, Y. Li, Z. Zou, H. Zhang, H. Xu, D. Xia, Appl. Surf. Sci. **439**, 697 (2018).